

## Interface view of directed sandpile dynamics

Chun-Chung Chen and Marcel den Nijs

*Department of Physics, University of Washington, P.O. Box 351560, Seattle, Washington 98195-1560*

(Received 30 March 2001; published 5 March 2002)

We present a directed unloading sand-box-type avalanche model, driven by slowly lowering the retaining wall at the bottom of the slope. The avalanche propagation in the two-dimensional surface is related to the space-time configurations in one-dimensional Kardar-Parisi-Zhang (KPZ) interface growth. We relate the scaling exponents of the avalanche cluster distribution to those for the growing surface. The numerical results are close but deviate significantly from the exact KPZ values. This might reflect stronger than usual corrections to scaling or be more fundamental, due to correlations between subsequent space-time interface configurations.

DOI: 10.1103/PhysRevE.65.031309

PACS number(s): 45.70.Ht, 05.65.+b, 05.70.Np, 47.54.+r

Avalanche phenomena are common in nature [1]. They are characterized by fast relaxation dynamics under a slow driving force. Models that describe such dynamics, e.g., so-called sandpile models, have been studied extensively for more than a decade following the work of Bak *et al.* [2]. Directed sandpile models are a special subclass in which relaxation follows a directional rule [3], that is, the propagation of active sites occurs only in one direction and never backfires. The central issue in this type of research is whether the dynamics is critical, such that the avalanche distribution functions are scale invariant (with power-law decay), and if so, whether these scaling properties are universal in the same sense as equilibrium critical phenomena. Our understanding of these issues is still restricted. There are only a few exactly soluble models, e.g., some deterministic Abelian directed sandpile models [3], but most insight is still limited to numerical simulation data. The evidence for scaling and universality in other types of nonequilibrium dynamics is less ambiguous: In surface growth (another example of intrinsic critical behavior) several universality classes are well established; e.g., Edwards-Wilkinson [4] and Kardar-Parisi-Zhang (KPZ) [5] type surface growth; population and catalysis type dynamics undergo absorbing-state-type phase transitions with distinct universality classes, such as directed percolation and directed Ising [6–8].

Efforts are under way to link avalanche dynamics to these better understood processes. This ranges from mappings to driven interfaces [9–11] and directed percolation [12,13], to direct appeals to concepts, such as universality [14,15,10] and renormalization [16,17]. Unfortunately the results remain confusing. In this paper we introduce a two-dimensional (2D) directed avalanche model with clear links to KPZ-type surface growth in one lower dimension (1D). For the latter, the scaling exponents are exactly known but nontrivial, such that the core issues become more translucent.

The physical system we have in mind is a sand box with a movable retaining wall to let out sand from the bottom of the slope, see Fig. 1. The retaining wall is lowered very slowly, such that grains tumble out sporadically forming distinct avalanches instead of a continuous flow. We model the sand surface by continuous height variables  $h(x,y)$ , with respect to a 2D square lattice, which is rotated over  $45^\circ$ , meaning that in the even (odd)  $y$  rows  $x$  takes only even (odd)

integer values. The retaining wall is placed at the  $y=0$  boundary. The slope is stabilized by the following constraint. The surface particle in column  $(x,y)$  is supported by the two columns  $(x\pm 1,y-1)$  just below it, and must be lower than the lowest of the two increased by a constant amount  $s_c$ ,

$$h(x,y) \leq \min[h(x+1,y-1), h(x-1,y-1)] + s_c. \quad (1)$$

The constant  $s_c$  can be set equal to 1 without loss of generality. An avalanche is triggered by selecting the highest site  $(x_i,0)$  at the  $y=0$  wall boundary (it is the  $i$ th avalanche) and reducing its height by a random amount,  $0 < \eta_i < s_c$ . This represents the lowering of the retaining wall. Next, all sites that violate the stability condition topple according to the rule

$$h(x,y) \rightarrow \min[h(x+1,y-1), h(x-1,y-1)] + \eta_i(x,y), \quad (2)$$

where  $0 < \eta_i(x,y) \leq s_c$  are uncorrelated random numbers. This toppling continues until the whole system is stable again. Since the toppling of a site in row  $y$  can only effect the stability of two sites immediately above it in row  $y+1$ , the sites can be updated row by row starting from the  $y=0$  boundary.

This process is idealized compared to a real unloading sand box in the sense that the toppled grains drop out without

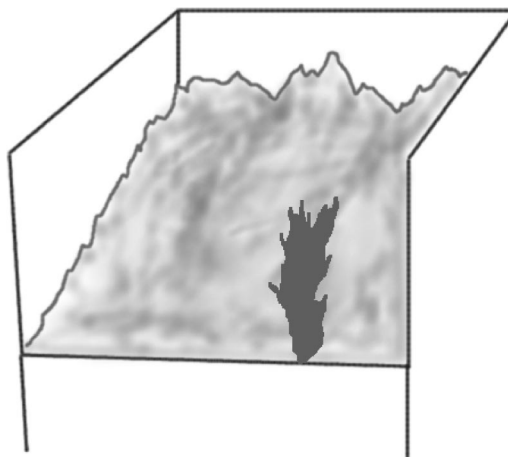


FIG. 1. Sand box with a slowly lowering retaining wall.

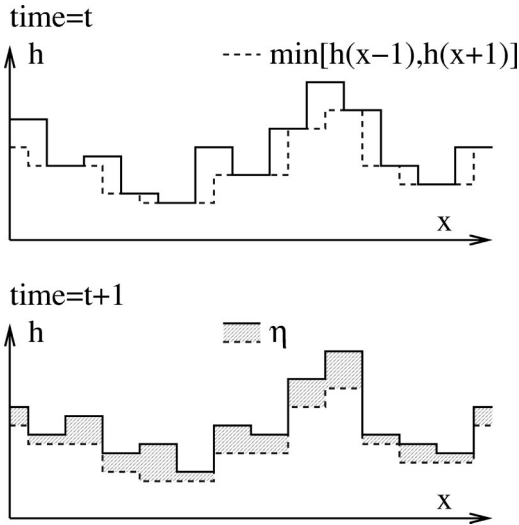


FIG. 2. KPZ-type growth dynamics.

disturbing the already stabilized lower regions of the surface. It is possible to justify this as the low gravity or strong bond limit where the falling sand does not gain enough momentum to disturb the stabilized surface on its way out. This is a nondissipative self-organized criticality (SOC) process. In more conventional examples, the avalanche is triggered by the deposition of a particle, and the toppling rule conserves particles. In our model, the slope plays this role. Lowering the retaining wall increases the slope at the bottom of the hill, and the avalanches conserve but propagate this change uphill.

The row-by-row toppling sequence (2) can be reinterpreted as the dynamic rule for a 1D growing interface, in which the  $y$  coordinate plays the role of time. Every stable surface configuration represents a world sheet of the 1D interface. Imagine creating an initial stable surface configuration, before the retaining wall starts to drop: choose an arbitrary configuration with all  $0 < h(x,0) \leq s_c$  in row  $y=0$ . Next, apply Eq. (2) to all sites in the next row,  $y=1$ , to create the next slice of the surface. Repeat this for all higher rows. The configuration in every row is similar to a 1D interface evolving in time  $t=y$ . Figure 2 illustrates how this interface propagates during each time step,  $y \rightarrow y+1$ . The upper panel shows the first half of the update (the drawn to the dashed line). This is the deterministic part of the propagation (the  $\min[\ ]$  operator) in Eq. (2). The lower panel illustrates the second half of the update, where the heights increase by a random amount  $0 < \eta \leq s_c$ . The first step removes material, and the second step deposits particles.

This type of interface dynamics almost certainly belongs to the KPZ universality class. Equation (2) can be rewritten as

$$h(x,t) = \frac{1}{2}[h(x+1,t-1) + h(x-1,t-1)] - \frac{1}{2}|h(x+1,t-1) - h(x-1,t-1)| + \eta(x,t), \quad (3)$$

which is a discrete version of the KPZ Langevin equation [5]

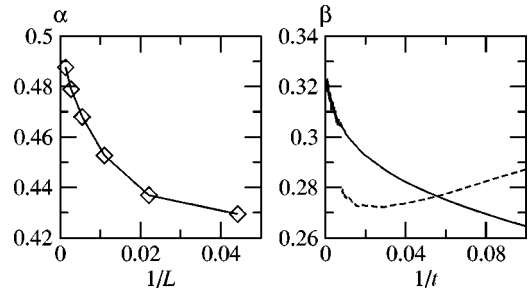


FIG. 3. Monte Carlo (MC) results for the global interface width: (a) finite size  $L_x$  estimates for the saturated surface width exponent  $\alpha$ ; (b) finite time estimates for the transient surface width exponent  $\beta$  from a flat initial configuration. The solid lines represent conventional MC simulations with an uncorrelated world sheet ensemble, and the dashed line is data from avalanche correlated MC runs.

$$\frac{\partial h}{\partial t} = \nabla^2 h - \frac{\lambda}{2} (\nabla h)^2 + \eta. \quad (4)$$

To be absolutely sure, and also to make sure that  $\lambda$  is large enough such that corrections to scaling from the EW point (at  $\lambda=0$ ) do not interfere, we checked numerically the behavior of the surface width  $\Delta(L,t)$ , defined as  $\Delta^2 \equiv \langle (h - \langle h \rangle)^2 \rangle$ . Starting from a flat surface at  $y=0$ , the width increases as  $\Delta \sim t^\beta$  for  $0 \leq t \leq L^z$  and saturates at  $\Delta \sim L^\alpha$  for  $t \gg L^z$ , with  $L$  the lattice size in the  $x$  direction. The numerical results in Fig. 3 are consistent with the exactly known KPZ values  $\alpha = \frac{1}{2}$ ,  $\beta = \frac{1}{3}$ , and  $z = \alpha/\beta = \frac{3}{2}$ .

We will present all our numerical results as finite size scaling (FSS) plots of effective exponents, e.g.,  $\alpha(L)$  in Fig. 3(a), obtained from applying the form  $\Delta = AL^\alpha$  to two nearby values of  $L$ . It is more common to present log-log plots, such as,  $\log(\Delta)$  versus  $\log(L)$ , and extract  $\alpha$  from a least-squares-type straight line fitting. That leads to results that appear statistically very accurate, but are systematically off when significant FSS corrections to scaling (subdominant power laws) are present [18]. Figure 3(a) is a good example of this. The approach to  $L \rightarrow \infty$  is consistent with a simple leading corrections to scaling power law with exponent  $y = -\frac{1}{2}$ .

The characteristic feature of the SOC is the lack of typical avalanche length, width, depth, or mass scales. The probability distributions follow power laws, as  $P_w \sim w^{-\tau_w}$  characterized by the scaling exponents,  $\tau_l, \tau_w, \tau_\delta$ , and  $\tau_m$ . Our numerical simulation results confirm the existence of scale invariance. The critical exponents converge well, see Fig. 4. The length  $l$  is the maximum  $y$  coordinate the avalanche reaches. The width  $w$  is the maximum departure in the  $x$  direction  $|x-x_i|$  from the trigger point  $x_i$ . The depth  $\delta$  is the maximum height change,  $h_i - h_{i-1}$ , caused by the avalanche, and the mass is the total amount of sand carried off by the avalanche.

The metadistribution function  $P(l,w,\delta)$  should obey the scaling form

$$P(l,w,\delta) = b^{-\sigma} P(b^{-z}l, b^{-1}w, b^{-\alpha}\delta), \quad (5)$$

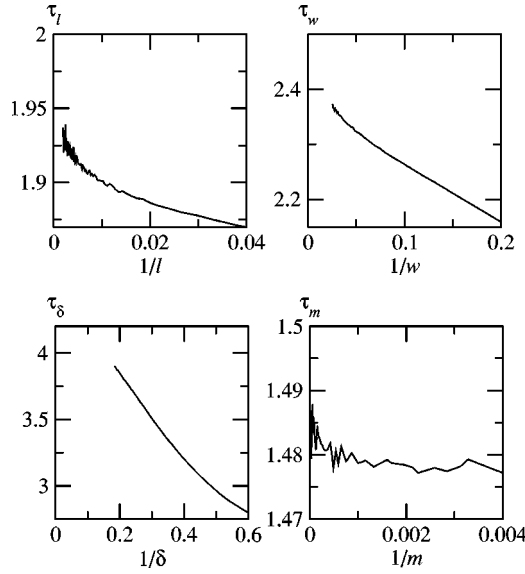


FIG. 4. Finite size scaling estimates of the avalanche distribution exponents,  $\tau_l$ ,  $\tau_w$ ,  $\tau_\delta$ , and  $\tau_m$ .

with  $b$  an arbitrary scale parameter. The exponents  $\sigma$ ,  $z$ , and  $\alpha$ , are expected to be robust with respect to details of the dynamic rule, and thus define the universality class. Single parameter distributions, such as,  $P_w \sim w^{-\tau_w}$ , follow by integrating out the other two parameters. This implies the following expressions for the  $\tau$  exponents:

$$\tau_l = \frac{\sigma - 1 - \alpha}{z}, \quad \tau_w = \sigma - z - \alpha, \quad \tau_\delta = \frac{\sigma - 1 - z}{\alpha}, \quad (6)$$

or inverted

$$z = \frac{\tau_w - 1}{\tau_l - 1}, \quad \alpha = \frac{\tau_w - 1}{\tau_\delta - 1}, \quad \sigma = \tau_w + z + \alpha. \quad (7)$$

Every stable slope configuration represents a possible world sheet of a 1D KPZ-type interface, and every avalanche the difference between two such world sheets. Therefore, it is natural to expect that the length (depth) of the avalanche scales with the KPZ value for  $z(\alpha)$ . In Fig. 5 we replot the numerical finite size scaling estimates of the  $\tau$  exponents in terms of  $\alpha$ ,  $z$ , and  $\sigma$ . The values  $z = 1.52 \pm 0.02$  and  $\alpha = 0.46 \pm 0.01$  are close to those of 1D KPZ growth, but in both cases the FSS curves overshoot the KPZ values and raise some serious doubts. The distribution of avalanche cluster sizes is the most commonly studied and experimentally the most accessible property of SOC. Its exponent is linked to  $\alpha$  and  $z$  in the following manner. At the start of the avalanche, the height of a boundary site ( $y=0$ ) is lowered on average by  $\frac{1}{2}s_c$ . Thus, for a sand box of width  $L_x$  the boundary row is lowered by  $\frac{1}{2}s_c$  after  $L_x$  avalanches. In the stationary state, the entire surface moves down on average by  $\frac{1}{2}s_c$  and the average amount of removed sand is equal to  $L_y \times \frac{1}{2}L_x s_c$ . Thus, the average mass of an avalanche must be equal to

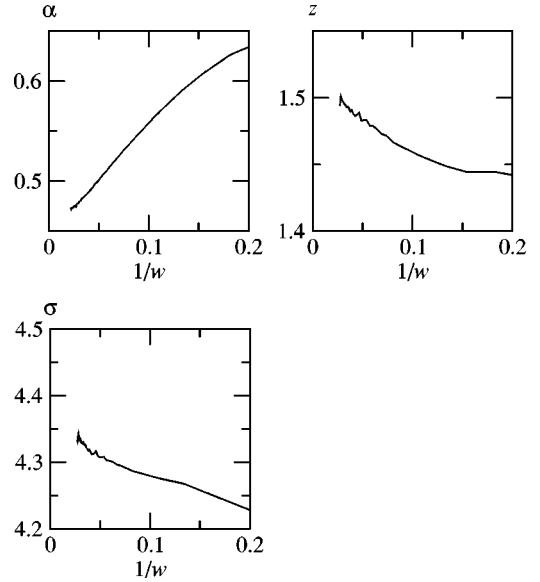


FIG. 5. Finite size scaling estimates for  $\alpha$ ,  $z$ , and  $\sigma$  derived from data in Fig. 4 using Eq. (7).

$$\langle m \rangle = \int dm m P_m(m) = \frac{1}{2} s_c L_y. \quad (8)$$

This is analogous to conservation of current in conventional deposition-type avalanche systems (see, e.g., [3]). Assume that the avalanche clusters are compact, i.e., the sizes of holes of unaffected regions inside an avalanche do not scale with the avalanche size. In that case, the mass scales as  $m \sim lw\delta$ , and we can use the metadistribution function to evaluate Eq. (8), as

$$\begin{aligned} \langle m \rangle \sim & \int_0^{L_y} dl \int_0^\infty dw \int_0^\infty d\delta lw \delta P(l, w, \delta) \\ & + m_{L_y} \int_{L_y}^\infty dl \int_0^\infty dw \int_0^\infty d\delta P(l, w, \delta). \end{aligned} \quad (9)$$

This applies when the box is wide and deep enough that  $L_y$  is the only limiting factor to the avalanches. The first term accounts for all avalanches that fit inside the box, and the second term for the ones that reach the  $L_y$  edge and thus are prematurely terminated. The first integral scales as  $L_y^{(-\sigma+2+2z+2\alpha)/z}$  for large  $L_y$ , while the second one scales as  $L_y^{(-\sigma+1+z+\alpha)/z}$ . We have assumed  $m \sim lw\delta$  so  $m_{L_y} \sim L_y^{(1+z+\alpha)/z}$ . The two terms in Eq. (9) scale in the same way, as

$$\langle m \rangle \sim L_y^{(-\sigma+2+2z+2\alpha)/z}. \quad (10)$$

Solving Eqs. (8) and (10) for  $\sigma$  gives

$$\sigma = 2 + z + 2\alpha. \quad (11)$$

This relation is numerically well satisfied. The direct measurement yields  $\sigma = 4.43 \pm 0.05$ , see Fig. 5, in mutual agreement with the numerical values for  $\alpha$  and  $z$ .

The intriguing issue we are left with is whether the slight but systematic deviations of the exponents in Fig. 5 from their KPZ values ( $\alpha = \frac{1}{2}$ ,  $z = \frac{3}{2}$ , and  $\sigma = \frac{9}{2}$ ) is for real or just an artifact of much stronger FSS corrections than usual (the avalanches cover only a small part of the surface). Conventional KPZ dynamics implies an ensemble average over independent Monte Carlo (MC) runs, i.e., over a large set of independent world sheets. The avalanche dynamics performs this ensemble average in a correlated manner. All subsequent world sheets are identical except for the avalanche area. This might change the scaling exponents and prove to be a key feature in how surface growth dynamics relates to avalanche-type SOC in general. To check this directly, the dashed curve in Fig. 3b shows the time evolution of the global KPZ surface roughness using avalanche correlated MC runs. The exponent  $\beta = \alpha/z$  is again consistent with the above avalanche scaling exponents and is systematically smaller than the KPZ value  $\beta = \frac{1}{3}$ . Maybe the upswing in the FSS estimates at large  $t$  indicates that the KPZ values are restored in the thermody-

namic limit, but this is a long shot. This issue needs further study, in particular, from an analytic KPZ perspective. For example, it is well known that (the somewhat analogous) correlated noise changes the KPZ exponents.

Finally, the exponent relations Eq. (7) apply also to the recent results of stochastic directed sandpile models by Paczuski and Bassler [19] and Kloster *et al.* [20] where the avalanche dynamics is related to Edwards-Wilkinson [4] surface growth, with  $z=2$  and  $\alpha=1/2$ ; and also to the exactly soluble directed sandpile model of Dhar and Ramaswamy, which satisfies Eq. (7) with  $z=2$  and  $\alpha=0$ . Unfortunately, these models do not resolve the KPZ exponents issue, because they are intrinsically simpler than ours, such that there are no correlations between the stable configurations of the sandpile and thus neither among successive avalanches.

This research was supported by the National Science Foundation under Grant No. DMR-9985806.

- 
- [1] P. Bak, *How Nature Works: The Science of Self-organized Criticality* (Copernicus, New York, 1996).
- [2] P. Bak, C. Tang, and K. Wiesenfeld, Phys. Rev. Lett. **59**, 381 (1987).
- [3] D. Dhar and R. Ramaswamy, Phys. Rev. Lett. **63**, 1659 (1989).
- [4] S.F. Edwards and D.R. Wilkinson, Proc. R. Soc. London, Ser. A **381**, 17 (1982).
- [5] M. Kardar, G. Parisi, and Y.-C. Zhang, Phys. Rev. Lett. **56**, 889 (1986).
- [6] W. Kinzel, Ann. Isr. Phys. Soc. **5**, 425 (1983).
- [7] For a review see J. Marro and R. Dickman, *Nonequilibrium Phase Transitions in Lattice Models* (Cambridge University Press, Cambridge, 1996).
- [8] J.D. Noh, H. Park, and M. den Nijs, Phys. Rev. E **59**, 194 (1999).
- [9] K. Sneppen, Phys. Rev. Lett. **69**, 3539 (1992).
- [10] M. Paczuski and S. Boettcher, Phys. Rev. Lett. **77**, 111 (1996).
- [11] K.B. Lauritsen and M.J. Alava, e-print, cond-mat/9903346.
- [12] B. Tadić and D. Dhar, Phys. Rev. Lett. **79**, 1519 (1997).
- [13] A. Vázquez and O. Sotolongo Costa, J. Phys. A **32**, 2633 (1999).
- [14] A. Ben-Hur and O. Biham, Phys. Rev. E **53**, R1317 (1996).
- [15] A. Mehta, J.M. Luck, and R.J. Needs, Phys. Rev. E **53**, 92 (1996).
- [16] L. Pietronero, A. Vespignani, and S. Zapperi, Phys. Rev. Lett. **72**, 1690 (1994).
- [17] A. Vespignani, S. Zapperi, and L. Pietronero, Phys. Rev. E **51**, 1711 (1995).
- [18] C.-S. Chin and M. den Nijs, Phys. Rev. E **59**, 2633 (1999).
- [19] M. Paczuski and K.E. Bassler, Phys. Rev. E **62**, 5347 (2000).
- [20] M. Kloster, S. Maslov, and C. Tang, Phys. Rev. E **63**, 026111 (2001).